Oxytocin and Vasopressin Receptors in the Pouched Rat

Samanta Arenas[a], Angela R. Freeman[a], Bhupinder Singh[b], Alexander G. Ophir[*,a]

[a] *Cornell University, Department of Psychology, Ithaca, NY, 14853*
[b] *Cornell University, Department of Veterinary Medicine, Ithaca, NY, 14853*

Abstract

This is the abstract. It consists of two paragraphs.

Introduction

The neuropeptides, oxytocin (OT) and vasopressin (VP), have receptor distributions in the brain that can modulate a variety of social behaviors such as parental care, affiliation, and aggression, among other behaviors (Caldwell and Albers, 2015). The densities of their associated receptors, oxytocin (OTR) and vasopressin (V1aR and V1bR) receptors, are often species- and sex-dependent.

- What do we know about the distribution and relative densities of receptors (i.e. what can it tell us, what's been done on behavior?)

-How might life history differences play into patterning of central distribution of these receptors?

-What tends to be conserved?

-How does comparative analysis help? (Kelly and Ophir, 2015)

-Why did we do this study? What were we examining?

-We wanted to describe the presence and relative density of OTR and V1aR in pouched rat brains in males and females, to see if there were differences in presence and density between sexes

-We wanted to explore how the patterning of these receptors might differ from other rodents and see if it further supports the ideas found in the recent metaanalysis (Freeman et al., 2020)(see where pouched rats fall in this framework)

Methods

All work with animals was approved under the U.S. Army Medical Research and Materiel Command (USAMRMC) Animal Care and Use Review Office (ACURO) and the Cornell Institutional Animal Care and Use Committee (IACUC 2014-0043). All tissues were collected from wild-caught animals from Morogoro, Tanzania (6°49'49"S, 37°40'14"E). Prior to collection, animals were housed individually in standard rabbit enclosures and

*Corresponding Author
Email addresses: sa658@cornell.edu (Samanta Arenas), arf86@cornell.edu (Angela R. Freeman), bs256@cornell.edu (Bhupinder Singh), ophir@cornell.edu (Alexander G. Ophir)

maintained on a 12:12 h light:dark light cycle, at 21°C and 45% humidity. Males and females were kept in separate rooms. Animals were fed a standard rodent diet supplemented with dog kibble and fresh fruit and vegetable treats. Chewing bones, a metal 'stovepipe' hutch, and dog puzzle toys were given as behavioral enrichment. Newspaper was given for nesting material.

Animals were euthanized via CO_2 inhalation and brains were swiftly removed and frozen using liquid nitrogen or powdered dry ice and stored at -80°C prior to sectioning. Ten male and ten female brains were used for this study. Brains were blocked coronally by removing the cerebellum, then split sagittally next to the midline into two hemispheres, and one hemisphere (preferably the left if unblemished) was coronally sectioned at 20µm thick using a Leica cryostat (CM1950, Leica Biosystems, Nussloch, Germany) set at -20°C. Due to the large size of the pouched rat brains, we mounted every 3rd section and kept 6 serial sets. Sections were collected from the olfactory bulbs to the start of the cerebellum, and mounted on Superfrost Plus Microscope sides (Fisher Scientific, Pittsburg, PA USA).

Microscope slides were stored at -80°C until the autoradiography procedure.

On two of the sets of slides, we used ^{125}I radioligands to label oxytocin receptor (ornithine vasopressin analog, ^{125}I-OVTA); NEX 254, PerkinElmer; Waltham, MA) or vasopressin 1a receptor (vasopressin (Linear), V-1A antagonist (Phenylacetyl1, 0-Me-D-Tyr2 [^{125}I-Arg6]-); NEX 310, PerkinElmer), as described by Ophir and colleagues (Ophir et al., 2013). Following processing and air-drying, we exposed radiolabeled tissue to film (Kodak Carestream Biomax MS) for 6 days for OTR and 2 days for V1aR to account for differing degrees of decay at the time of use. In each film cassette, we included two ^{125}I microscales (American Radiolabeled Chemicals; St Louis, MO), to allow for the conversion of optical density to receptor density. We inferred that receptor density relates to optical density of exposed film to use optical measurements as a proxy for receptor density. We digitized films on a Microtek ArtixScan M1 (Microtek, Santa Fe Springs, CA) and measured optical densities using NIH ImageJ Software. We calculated receptor density by first converting optical density to disintegrations per minute (dpm), adjusted for tissue equivalence (TE; for 1 mg in the rat brain), by fitting curves generated by radiographic standards and extrapolating based on these standard curves for each film.

Three sequential sections were measured for density by encircling the regions of interest using NIH ImageJ software. The software program calculated mean optical density values and area for regions of interest (ROI). We measured background labelling by measuring optical density from an area of cortex in the same section for each region of interest. To correctly identify ROI, we Nissl-stained a third set of tissue to use as a reference, in conjunction with anatomical landmarks identified using a Rat brain atlas. The three measurements for each individual's ROIs and background were averaged separately, and background was subtracted from the ROI to yield receptor density. These final measurements were used for all statistical tests, tables, and figures.

OTR density was measured in the olfactory bulb (OB), anterior olfactory nucleus (AON), prefrontal cortex (PFC), piriform cortex (Pir), nucleus accumbens (NAcc), lateral septum (LS), endopiriform (Den), claustrum

(VCL), lateral bed nucleus of the stria terminalis (BSTl), medial bed nucleus of the stria terminalis (BSTm), ventral bed nucleus of the stria terminalis (BSTv), ventral pallidum (VPall), medial preoptic area (MPOA), anterior hypothalamus (AH), paraventricular thalamus (PVT), suprachiasmatic nucleus (SCN), paraventricular nucleus (PVN), magnocellular hypothalamic nucleus (MCPO), medial habenula (MHb), central amygdala (CeA), medial amygdala (MeA), basolateral amygdala (BLA), ventromedial hypothalamus (VMH), zona incerta (ZIR), lateral hypothalamus (PrFLH), hippocampal CA1, hippocampal CA2, hippocampal CA3, dentate gyrus (DG), premammilary ventral nucleus (PMV), ventral tegmental area (VTA), periaqueductal gray (PAG), medial geniculate (MG), superior colliculus (SuG), and the ventral CA3. V1aR was measured in the same regions except for the MCPO and the MHb.

To calculate 'relative binding' on a 4-point scale, we used the following definitions: mean OTR < 35 dpm/mg: absent/-, 35 to 490: present/+, 490 to 945: moderate/++, 945 to 1400: dense/+++; mean V1aR < 100 dpm/mg: absent/-, 100-1367: present/+, 1367 to 2634: moderate/++, 2634 to 3800: dense/+++. To compare receptor densities between sexes, we conducted t-tests for each region. We used a bonferroni correction to adjust for multiple comparisons. Test statistics were considered significant when $p < 0.05$.

We used the framework from Freeman et al. (2020) to compare pouched rat overall binding patterns to those in other rodents (Freeman et al., 2020). This framework uses overall OTR and V1aR binding patterns to examine similarities among species, genera, and family groups. Briefly, relative binding patterns within a species are converted to a 4-point scale, using wording and data from previously published studies. These data are then used in a principal components analysis, and species are plotted along the PC1 and PC2 components, with vectors in the plot serving as weights of each variable, and the direction indicating loading on PC1 and PC2.

We mapped pouched rat relative binding data onto this plot based on this framework and the data presented in this study. In addition to superimposing the pouched rat onto the PCA biplot, we recreated the comparative permutational anova (Adonis function) to examine whether genus or family groups predicted similarities among species' relative binding patterns. All analyses were conducted in R 4.0.2, with the vegan package for the 'adonis' function, and stats package for t tests and principal components analysis (R Development Core Team, 2016). PCA biplots were made using the ggbiplot function in the ggbiplot package with some aesthetic changes.

Results

After comparing male and female densities in the measured regions, most regions showed no differences between sexes. The superior colliculus had higher densities of OTR in females compared to males (Table 1, Female mean: 199.35, Male mean 51.46, $t_{(13.58)} = 2.79$, $p = 0.01$), however, this was no longer significant after corrections for multiple comparisons (adjusted $\alpha = 0.001$).

Table 1: OTR densities by region and sex

Region	Sex	Density mean ± SE (dpm/mg)	N
Olfactory Bulb	F	126.27 ± 39.56	9
Olfactory Bulb	M	142.74 ± 39.34	9
Accessory Olfactory Nucleus	F	186.38 ± 40.35	9
Accessory Olfactory Nucleus	M	144.1 ± 30.98	9
mPFC	F	117.96 ± 36.91	9
mPFC	M	94.51 ± 32.08	9
Infralimbic Cortex	F	138.22 ± 43.25	9
Infralimbic Cortex	M	72.54 ± 20.32	9
Nac Core	F	46.18 ± 14.48	9
Nac Core	M	37.34 ± 12.45	9
Nac Shell	F	81.44 ± 17.96	9
Nac Shell	M	51.75 ± 13.37	9
Caudate Putamen	F	30.8 ± 13.39	9
Caudate Putamen	M	23.93 ± 8.42	9
Piriform Cortex	F	222.05 ± 39.71	9
Piriform Cortex	M	192.1 ± 35.8	9
Lateral Septum I	F	55.24 ± 12.25	11
Lateral Septum I	M	57.94 ± 13.57	9
Lateral Septum D	F	48.7 ± 7.59	11
Lateral Septum D	M	56.22 ± 12.33	9
Lateral Septum V	F	71.16 ± 16.63	11
Lateral Septum V	M	103.53 ± 35.63	9
Endorpiriform Cortex	F	147.07 ± 22.53	10
Endorpiriform Cortex	M	111.82 ± 19.71	9
Claustrum	F	192.58 ± 47.69	10
Claustrum	M	193.17 ± 28.09	9
BSTm	F	585.91 ± 117.64	10
BSTm	M	532.58 ± 91.23	9
BSTi	F	687.03 ± 132.48	10
BSTi	M	425.66 ± 79.05	9
BSTv	F	101.57 ± 21.35	10

Region	Sex	Density mean ± SE (dpm/mg)	N
BSTv	M	92.97 ± 28.24	9
Ventral Pallidum	F	107.32 ± 15.18	10
Ventral Pallidum	M	78.04 ± 23.15	9
MPOA	F	95.77 ± 19.61	10
MPOA	M	88.22 ± 17.61	9
Anterior Hypothalamus	F	90.27 ± 24.22	10
Anterior Hypothalamus	M	74.19 ± 17.25	7
PVT	F	50.91 ± 16.77	10
PVT	M	64.52 ± 27.91	7
SCN	F	80.48 ± 23.44	10
SCN	M	125.57 ± 45.86	7
PVN	F	14.44 ± 16.18	9
PVN	M	93.85 ± 41.77	7
Medial Hypothalamic Nucleus	F	118.68 ± 37.66	9
Medial Hypothalamic Nucleus	M	122.42 ± 33.6	7
Medial Habenula	F	545.93 ± 121.71	10
Medial Habenula	M	648.41 ± 97.33	9
Central Amygdala	F	695.23 ± 144.28	9
Central Amygdala	M	734.04 ± 92.77	9
Medial Amygdala	F	328.84 ± 51.14	9
Medial Amygdala	M	380.99 ± 82.29	9
Basolateral Amygdala	F	627.27 ± 120.17	9
Basolateral Amygdala	M	712.9 ± 155.24	9
VMH	F	1242.79 ± 245.41	9
VMH	M	1224.42 ± 165.26	9
Zona Incerta	F	408.51 ± 67.31	10
Zona Incerta	M	415.41 ± 58.07	9
Lateral Hypothalamus	F	176.03 ± 32.85	10
Lateral Hypothalamus	M	171.5 ± 41.95	9
CA1	F	121.81 ± 25.41	11
CA1	M	107.19 ± 15.49	9
CA2	F	106.13 ± 11.57	11

Region	Sex	Density mean ± SE (dpm/mg)	N
CA2	M	127.54 ± 25.3	9
CA3	F	39.48 ± 10.47	11
CA3	M	45.77 ± 10.29	9
Premammillary Nucleus	F	535.99 ± 110.84	10
Premammillary Nucleus	M	499.3 ± 106.84	9
VTA	F	523.97 ± 74.13	9
VTA	M	628.2 ± 174.1	9
PAG	F	191.21 ± 35.76	10
PAG	M	106.35 ± 28.22	7
Superior Colliculus	F	199.35 ± 46.21	10
Superior Colliculus	M	51.46 ± 26.08	7

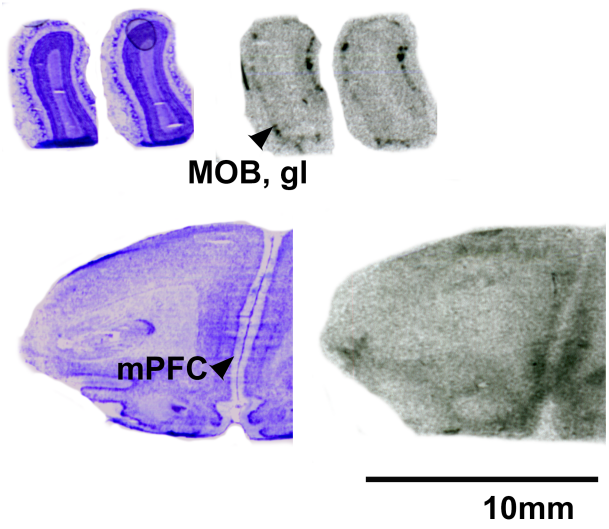

Figure 1: OTR in the forebrain of the pouched rat

Pouched rats had very dense binding in the VMH, with moderate binding in the BST, CeA and VTA. There was only a low level of binding in the OB and mPFC (Table 2, Figure 1).

Table 2: OTR relative densities in select regions

Region	Relative.Binding
Olfactory Bulb	+
Nucleus Accumbens	+
mPFC	+
Ventral Pallidum	-
Lateral Septum	+
BST	++
CeA	++
MeA	+
Hippocampus	+
VMH	+++
VTA	++

Table 3: V1aR densities by region and sex

Region	Sex	Density mean ± SE (dpm/mg)	N
Olfactory Bulb	F	1456.47 ± 244.89	9
Olfactory Bulb	M	1841.49 ± 278.59	8
Accessory Olfactory Nucleus	F	1287.3 ± 173.38	9
Accessory Olfactory Nucleus	M	1596.88 ± 235.76	8
mPFC	F	588.16 ± 73.53	11
mPFC	M	604.41 ± 115.62	9
Infralimbic Cortex	F	388.15 ± 52.78	11
Infralimbic Cortex	M	426.68 ± 111.74	9
Nac Core	F	1319.1 ± 113.88	11
Nac Core	M	1748.56 ± 266.36	8
Nac Shell	F	1389.26 ± 169.07	11
Nac Shell	M	1687.58 ± 362.54	9
Caudate Putamen	F	1725.67 ± 148.69	11
Caudate Putamen	M	2329.94 ± 322	9
Piriform Cortex	F	604.16 ± 87.76	11
Piriform Cortex	M	649.05 ± 144.85	9
Lateral Septum I	F	3602.8 ± 355.47	11
Lateral Septum I	M	2885 ± 369.04	9
Lateral Septum D	F	3451.24 ± 276.7	11
Lateral Septum D	M	3613.44 ± 207.77	9
Lateral Septrum V	F	2395.85 ± 311.31	11
Lateral Septrum V	M	2351.65 ± 325.22	9
Endopiriform Cortex	F	296.6 ± 58.56	11
Endopiriform Cortex	M	260.42 ± 57.86	9
Claustrum	F	446.08 ± 74.68	11
Claustrum	M	334.95 ± 58.2	9
BSTm	F	1552.05 ± 161.04	11
BSTm	M	1452.1 ± 229.77	9
BSTi	F	1297.66 ± 80.59	11
BSTi	M	1056.38 ± 188.24	9
BSTv	F	885.07 ± 108.44	11

Region	Sex	Density mean ± SE (dpm/mg)	N
BSTv	M	835.57 ± 116.42	9
Ventral Pallidum	F	616.94 ± 104.42	11
Ventral Pallidum	M	470.4 ± 142.24	9
MPOA	F	626.46 ± 84.5	11
MPOA	M	522.26 ± 75.01	9
Anterior Hypothalamus	F	364.98 ± 97.49	9
Anterior Hypothalamus	M	601.09 ± 288.18	8
PVT	F	63.75 ± 58.22	9
PVT	M	245.11 ± 131.63	8
SCN	F	207.91 ± 109.3	9
SCN	M	85.55 ± 71.97	8
PVN	F	514.58 ± 146.84	8
PVN	M	520.91 ± 161.33	7
Central Amygdala	F	1710.61 ± 186.92	10
Central Amygdala	M	1439.79 ± 188.75	9
Medial Amygdala	F	841.82 ± 76.12	10
Medial Amygdala	M	928.64 ± 160.08	9
Basolateral Amygdala	F	120.35 ± 66.19	10
Basolateral Amygdala	M	139.62 ± 74.36	9
VMH	F	390.55 ± 130.5	10
VMH	M	576.42 ± 141.68	9
Zona Incerta	F	705.31 ± 78.81	10
Zona Incerta	M	738.07 ± 94.39	9
Lateral Hypothalamus	F	745.93 ± 91.88	10
Lateral Hypothalamus	M	915.03 ± 143.4	9
CA2	F	119.25 ± 56.35	11
CA2	M	63.4 ± 81.27	9
Dentate Gyrus	F	281.61 ± 107.99	11
Dentate Gyrus	M	347.83 ± 172.25	9
Premammillary Nucleus	F	1458.58 ± 333.09	11
Premammillary Nucleus	M	2206.81 ± 616.26	9
VTA	F	1132.57 ± 186.43	11

Region	Sex	Density mean ± SE (dpm/mg)	N
VTA	M	1278.42 ± 203.04	9
PAG	F	734.99 ± 97.71	11
PAG	M	947.68 ± 293.67	7
Medial Geniculate	F	93.87 ± 50.87	11
Medial Geniculate	M	147.82 ± 117.32	7
Superior Colliculus	F	819.1 ± 146.2	11
Superior Colliculus	M	744.4 ± 229.16	7
Ventral CA3	F	67.1 ± 78.53	5
Ventral CA3	M	119.62 ± 148.52	2

Table 4: V1aR relative densities in select regions

Region	Relative.Binding
Olfactory Bulb	++
Nucleus Accumbens	++
mPFC	+
Ventral Pallidum	+
Lateral Septum	+++
BST	++
CeA	++
MeA	+
PVN	+
Hippocampus	-
Dentate Gyrus	+
Premammillary Nucleus	++
VMH	+
VTA	+

-Where did we see binding for OTR

-Where did we see binding for V1aR

-Sex differences

-Predict with PCA

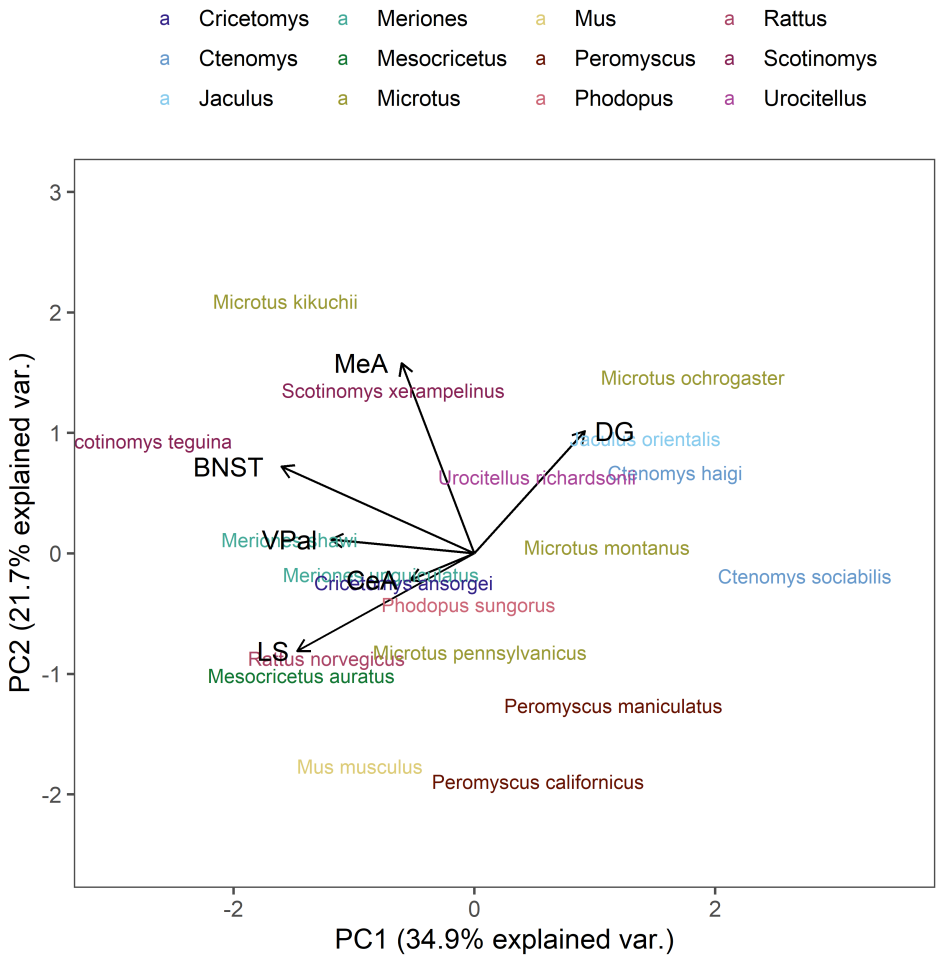

Figure 2: a PCA, V1aR with species maximized

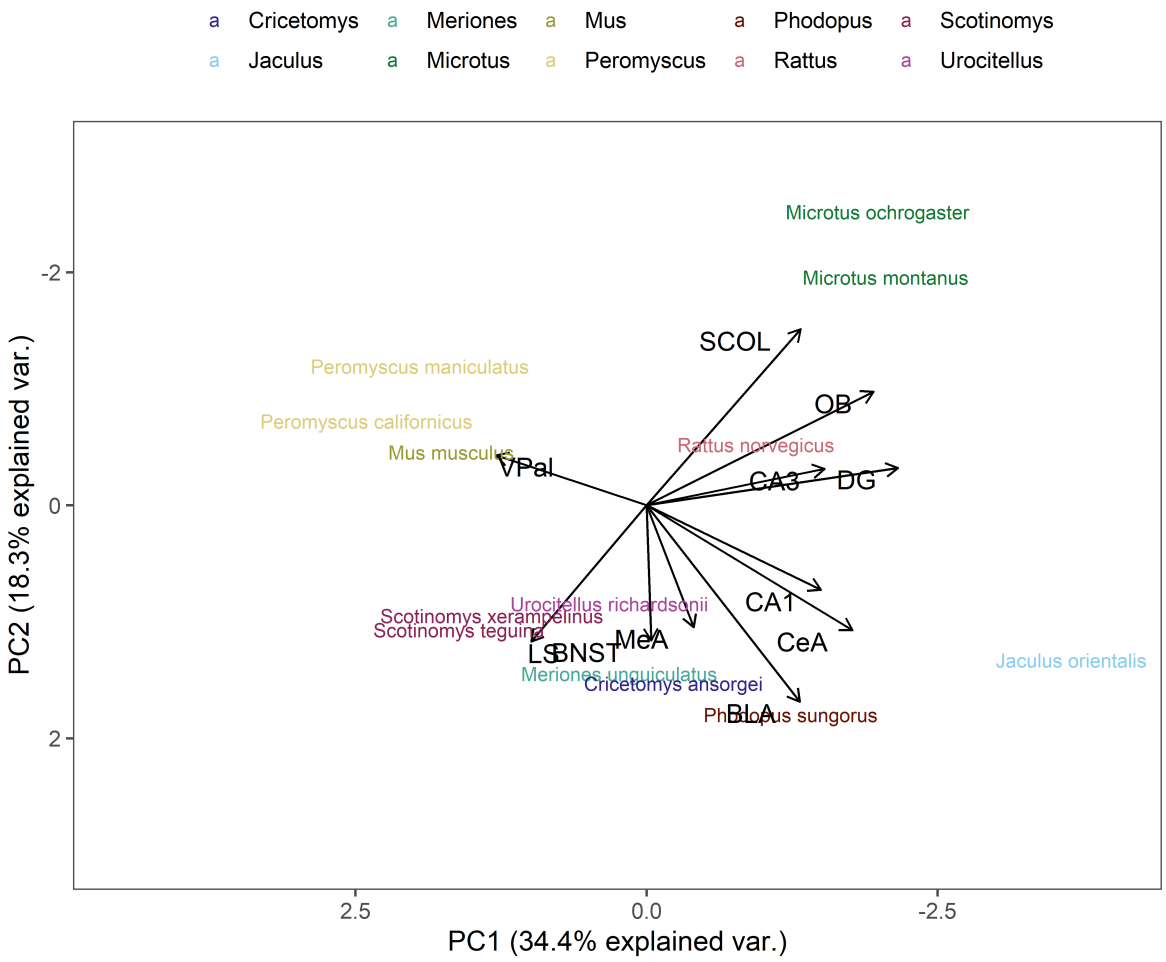

Figure 3: a PCA, V1aR with regions maximized

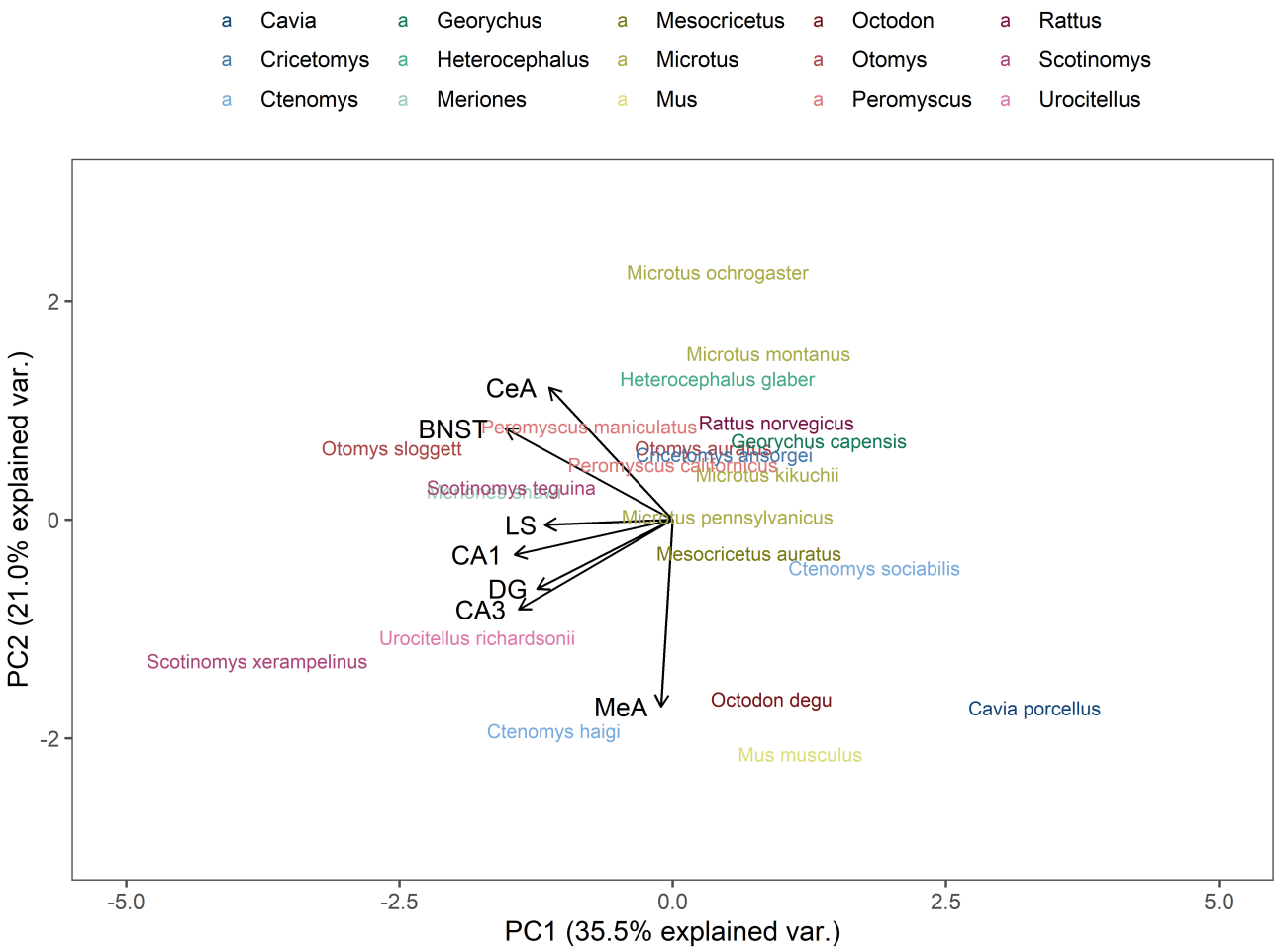

Figure 4: a PCA, OTR with species maximized

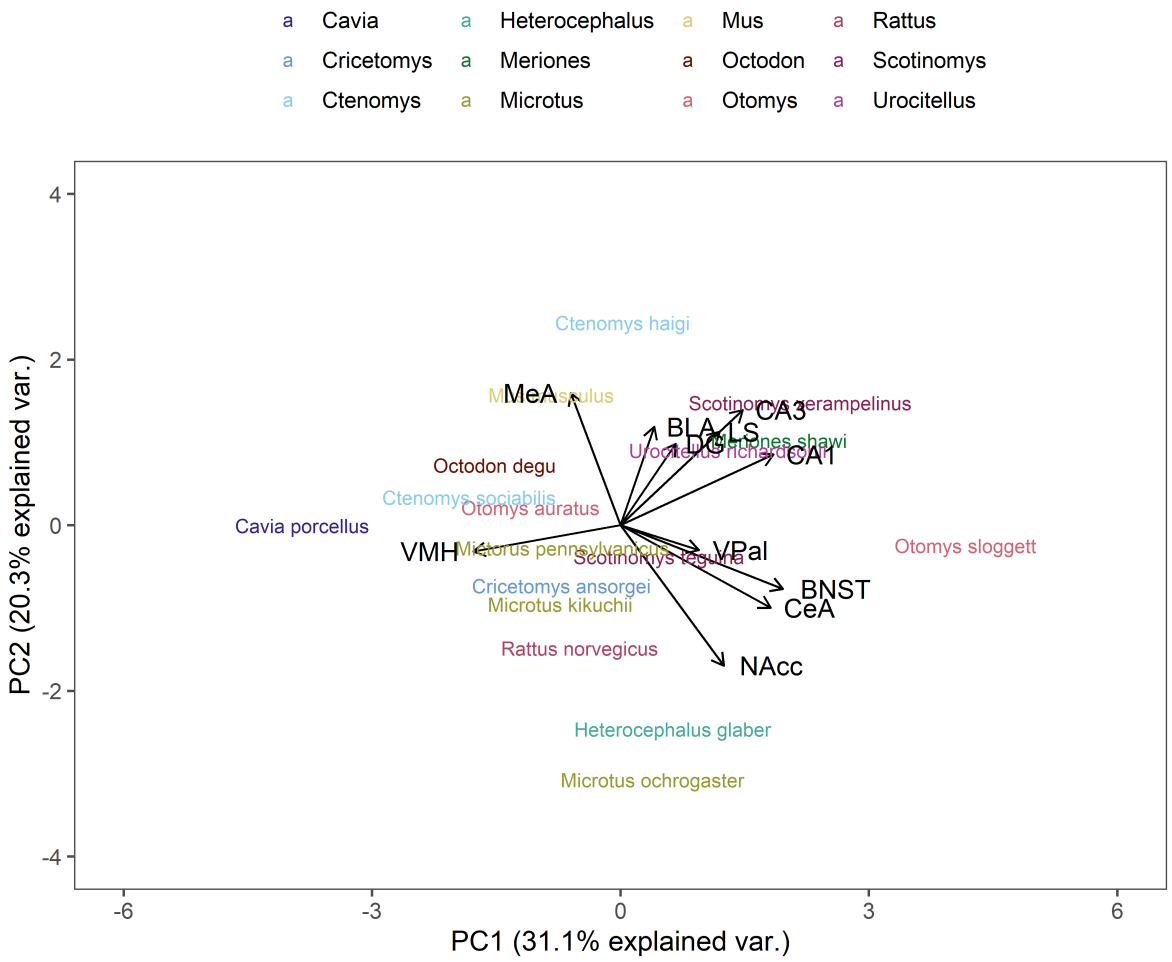

Figure 5: a PCA, OTR with regions maximized

Discussion

-We found OTR in ... V1aR in....

-Sex differences in densities/presence and absence

-We found that overall patterns were similar to.....

-Caveats

-Unknown age

-Unknown reproductive status

-Different experiences possible

-What this means, similarities to other species

-Relevance for behavior or life history

What still needs to be known?

References

Caldwell, H.K., Albers, H.E., 2015. Oxytocin, vasopressin, and the motivational forces that drive social behaviors, in: Behavioral Neuroscience of Motivation. Springer, pp. 51–103. doi:10.1007/7854

Freeman, A.R., Aulino, E.A., Caldwell, H.K., Ophir, A.G., 2020. Comparison of the distribution of oxytocin and vasopressin 1a receptors in rodents reveals conserved and derived patterns of nonapeptide evolution. Journal of Neuroendocrinology 32, e12828. doi:10.1111/jne.12828

Kelly, A.M., Ophir, A.G., 2015. Compared to what: What can we say about nonapeptide function and social behavior without a frame of reference? Curr Opin Behav Sci 6, 97–103. doi:10.1016/j.cobeha.2015.10.010

Ophir, A.G., Sorochman, G., Evans, B.L., Prounis, G.S., 2013. Stability and dynamics of forebrain V1aR and OTR during pregnancy in prairie voles. Journal of neuroendocrinology 25, 719–728. doi:10.1111/jne.12049

R Development Core Team, 2016. R: A language and environment for statistical computing. R Foundation for Statistical Computing, Vienna, Austria. URL http://www.R-project.org/., R Foundation for Statistical Computing, Vienna, Austria. doi:10.1007/978-3-540-74686-7